

# Bulk dipole contribution to second harmonic generation in diamond lattices\*

Hendradi Hardhienata<sup>†,1,2</sup> David Stifter,<sup>1,2</sup> Amirreza Baghbanpourasl,<sup>2</sup>

Andrii Prylepa,<sup>1,2</sup> Cornelia Reitböck,<sup>1,2</sup> and Kurt Hingerl<sup>2</sup>

<sup>1</sup>*Christian Doppler laboratory for microscopic and spectroscopic material characterization,  
Johannes Kepler University, Altenbergerstr. 69, 4040 Linz, Austria*

<sup>2</sup>*Center for surface- and nanoanalytics,  
Johannes Kepler University, Altenbergerstr. 69, 4040 Linz, Austria*

## Abstract

It is generally argued that material classes with inversion symmetry do not produce bulk dipole related second harmonic generation (SHG). So, SHG is then either ascribed to surface effects or bulk related electric quadrupole or magnetic dipole effects. Using symmetry and *ab-initio* potentials we show analytically that due to the fact of the decaying harmonic electric field certain diamond crystal orientations, as e.g. Si(111), produce a bulk dipole SHG response. For fcc and bcc lattices with a single atom basis, i.e. for the most important metals, however, SHG can purely arise due to the disturbance induced by the surface. Finally we propose an experiment, exploiting the different dispersion for the fundamental as well as frequency doubled radiation to determine this effect.

---

<sup>†</sup> on leave from Theoretical Physics Division, Institut Pertanian Bogor, Indonesia

The recent high interest in surface science techniques capable to probe surfaces *in-situ* has renewed the interest in linear and nonlinear optical techniques such as second harmonic generation (SHG). This interest has been accompanied by theoretical efforts to model the measured data, interpreting them either in a classical picture or taking into account quantum mechanics by involving transitions between initial and final states.<sup>1-6</sup> Especially for SHG the interpretation and the origin of the data is controversial. Some authors<sup>7-9</sup> claim that part of the SHG response arises from the surface and bulk quadrupoles or from magnetic dipole effects, whereas others<sup>10,11</sup> are mainly considering surface contributions. To our knowledge, however, all the literature has up to now neglected bulk dipole transitions in materials with inversion symmetry<sup>12-14</sup> using the following argument: Materials with inversion symmetry are described by potentials with even powers of the coordinates (i.e.  $\vec{r}^2$ ,  $\vec{r}^4$ , etc.). Because a second harmonic contribution providing response to an incident field oscillating with frequency  $\omega$  could origin, due to inversion symmetry, only from forces which are quadratic, or potentials which are cubic in a component of  $\vec{r}$ , this effect has been directly excluded. Analytically, the quantum mechanical expression for each tensor element of the second order susceptibility is<sup>15</sup>

$$\chi_{ijk}^{SHG} = \frac{Ne^3}{\epsilon_0 \hbar^2} \sum_{n,n'} \left( \frac{\langle j \rangle_{0n} \langle k \rangle_{nn'} \langle i \rangle_{n'0}}{(\omega_{n0} - \omega)(\omega_{n'0} - 2\omega)} + \frac{\langle k \rangle_{0n} \langle i \rangle_{nn'} \langle j \rangle_{n'0}}{(\omega_{n0} - \omega)(\omega_{n'0} + \omega)} + \frac{\langle i \rangle_{0n} \langle j \rangle_{nn'} \langle k \rangle_{n'0}}{(\omega_{n0} + 2\omega)(\omega_{n'0} + \omega)} \right). \quad (1)$$

In equ. (1)  $i, j, k$  denote  $x, y, z$ ,  $N$  the density of oscillators, and each sum runs over all intermediate states  $n, n'$ . Therefore for fcc and bcc lattices, as e.g. for Cu or Fe with a single atom basis, a symmetric potential and therefore well defined wavefunction parity, equ. (1) yields zero, because then product of uneven number of excitations cannot close the loop back to the original state (for details see equ. 8.40 in reference<sup>15</sup>).

To our knowledge it has never been discussed in the context of SHG that the potential of atoms in the diamond structure is, due to their tetrahedral bonding, intrinsically inversion asymmetric. This asymmetry can be observed by using a pictorial representation for the tetrahedral hybridized  $sp^3$  wavefunctions (Fig.1a), respectively by displaying the *ab initio* potential along the  $\langle 111 \rangle$  direction (Fig.1b), or by plotting the potential within in the (111) plane as equi-contour plot (Fig.1c). The potential has been calculated with the density functional theory implementation of VASP 5.2 using generalized gradient approximation (GGA). The interaction between the four electrons and the Si ion is described by projector augmented wave technique<sup>16</sup>. The constructed potential de-

scribing a fourfold ionized Si and four electrons is rather strong ( $\simeq -120\text{eV}$ ). The calculated electron energies, however, are of the order of a few eV, and therefore the electrons "feel" the asymmetry of the potential. Including the exchange correlation part makes the potential landscape even more asymmetric.

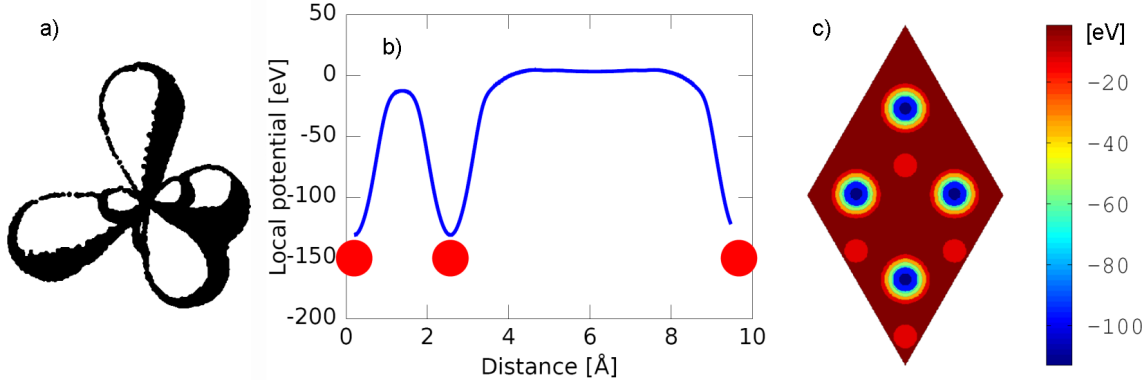


FIG. 1: a) Plot of the probability density for the  $sp^3$  hybridized wavefunctions for Si(111), b) *ab-initio* potential for Si (111) along the  $[111]$  direction. c) Contour plot of the *ab-initio* potential for Si in the (111) plane. The red dots represent the positions of the Si atoms.

Plotting the *ab-initio* potential through another plane, e.g. parallel to a Si(100) surface yields an inversion symmetric potential and so an electric field vector within this plane cannot excite SHG. However, because the polarization of the electric field can be in an arbitrary direction to the bonds, each Si atom will produce for an arbitrary polarization SHG response. Also for the case of Si(111), usually the SHG response will be minor, because two neighboring Si atoms form a symmetric entity, if there is no perturbation. So, in all static or long wavelength limit effects the SHG response of two neighboring Si atoms cancels, as well as for certain symmetries between the perturbing electric field and the crystallographic arrangement (e.g. normal incidence on Si(110) or Si(100)).

In the general case, however, when the amplitude of the electric field is different on both atom sites, the two responses **will not add up fully destructively and produce in the far field a measurable signal**. A strength variation of the electric field could either occur through strong (asymmetric) focusing, or which is discussed beneath, by the intrinsic absorption of the fundamental wave, when it propagates into the material. The effect of a varying amplitude of the *macroscopic* electric field can be either described by employing spatially dispersive (non-local) models, which means that the dielectric function depends on the wave-vector and the frequency as in ref.<sup>17</sup>, or,

as done recently, to derive within a classical bond model that spatial dispersion is proportional to the gradient of the macroscopic electric field along the bond<sup>9</sup>. Using bonds instead of the lattice positions disguises the symmetry properties of the underlying lattice and requires the use of classical mechanics. Therefore we will proceed by explicitly specifying the spatial dependence of the macroscopic electric fields. If a wave impinges perpendicular onto e.g. silicon with a (111) orientation (see FIG. 2a), the perturbation through the electric field  $\vec{E}$  can be significant.

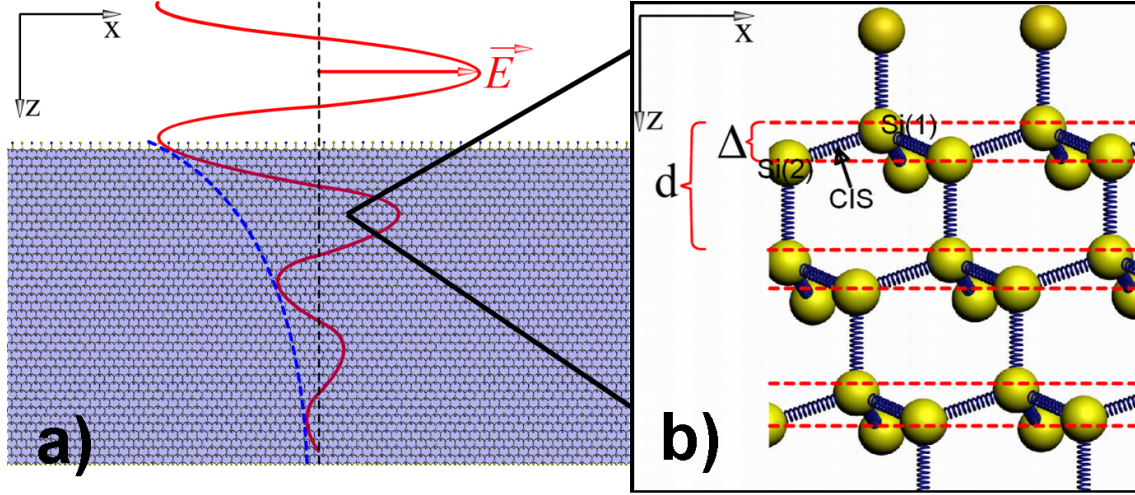


FIG. 2: a) The incoming electric field decays along the propagation direction. b) Layers are shown where one Si atom (Si(1)) is covalently bound to one from above and to three Si atoms underneath, where one is called Si(2). The center of inversion symmetry (CIS) is located in the middle between Si(1) and Si(2).

Si(111), respectively its atoms, can be described in a simple picture by four equivalent covalent bonds with a sequence of layers, which are alternately bound by one up bond or by three down bonds to the next layer (see FIG. 2b). For our model it is insignificant, if we imagine the bonds either as rigid, such that the electrons can only move along the bond direction<sup>11</sup> or as  $sp^3$ -hybridized orbitals<sup>18</sup>, or as extended coherent wavefunctions, describing the probability density for finding the electron in a given spatial interval. The electronic probability density is the same for positions around Si(1) respectively Si(2), which are at slightly different  $z$ - positions. **Therefore, the atoms experience a different field strength**, as indicated in FIG. 2a). So, in the antenna picture for the bulk (111) case the two waves, originating at Si(1) respectively Si(2) do not fully destructively interfere. The non-linear polarization for a single atom/layer (SL), either Si(1) or Si(2), is derived

72 by

$$P_i^{SL,2\omega} = \frac{\varepsilon_0}{2} \sum_{jk} \chi_{ijk}^{SL}(2\omega; \omega, \omega) E_j(\omega) E_k(\omega) \quad (2)$$

73 where  $\chi_{ijk}^{SL}$  stands for the specific coefficient of the nonlinear hyperpolarisability of a **single** Si  
 74 atom respectively layer. The nonlinear hyperpolarisability yields for a single Si(111) tetrahedron  
 75 a finite contribution as it has been found before for single  $sp^3$ -orbital<sup>18</sup>. For the case of the later  
 76 discussed simplified bond-hyperpolarisability (SBHM) model<sup>11</sup>  $\chi_{ijk}^{SL}$  can be easily found by setting  
 77 in the cited reference the up- and the down hyperbolarisabilities equal. When the fundamental  
 78 field penetrates through the bulk, it decays with a complex wavevector  $k = \omega\tilde{n}/c$ , respectively an  
 79 absorption coefficient  $\alpha_\omega/2$ , given by  $\alpha_\omega = \frac{4\pi n_i}{\lambda_0}$ , where  $\lambda_0$  is the vacuum wavelength, and  $n_i$  is the  
 80 imaginary part of the refractive index  $\tilde{n}$ , connected to the dielectric function  $\epsilon(\omega)$  by  $\epsilon(\omega) = \tilde{n}(\omega)^2$ .  
 81 **Because the exciting field decays along z due to absorption**, the response of the bonds of Si(1)  
 82 **does not fully cancel** the contribution of the lower atom Si(2). It has to be mentioned that even for  
 83 the case that the photon energy is smaller than half the bandgap, the occurrence of SHG implies  
 84 absorption of the linear wave. For a bond length in Si of  $\simeq 2.35\text{\AA}$  the period  $d$  of the slabs is  
 85  $\simeq 3.16\text{\AA}$  and the normal distance  $\Delta$  between the (1) and (2) atoms is  $\simeq 0.8\text{\AA}$ . We calculate the  
 86 difference of the radiated SHG field for one slab just beneath the surface ( $z = 0^+$ ) as the coherent  
 87 superposition of the Si(1) and Si(2) atom:

$$\begin{aligned} C_{(1)} &= (\text{Re}[e^{ik_\omega z}])^2 e^{-\alpha_\omega z} \text{Re}[e^{ik_{2\omega} z}] e^{-\alpha_{2\omega} z/2} \\ C_{(2)} &= (\text{Re}[e^{ik_\omega(z+\Delta)}])^2 e^{-\alpha_\omega(z+\Delta)} \text{Re}[e^{ik_{2\omega}(z+\Delta)}] e^{-\alpha_{2\omega}(z+\Delta)/2} \\ P_i^{slab,2\omega} &= \frac{\varepsilon_0}{2} \sum_{jk} \chi_{ijk}^{SL}(2\omega; \omega, \omega) (C_{(1)} - C_{(2)}) E_j^0(\omega) E_k^0(\omega) \end{aligned} \quad (3)$$

88 where the first equation yields the response of Si(1) at  $z$ , the second equation the response  
 89 of Si(2) at depth  $z + \Delta$ . We explicitly use real fields in the nonlinear process. The exponential  
 90 decaying terms in the field have to be squared in the nonlinear process, yielding the absorption  
 91 coefficient. Also the backward propagating wave with twice the fundamental frequency is damped,  
 92 which is then detected in vacuum or air. The third equation makes explicit use of spatial dispersion,  
 93 i.e. the field dependence, and  $E_j^0$  denotes the transmitted space independent fundamental electric  
 94 field amplitude at ( $z = 0^+$ ), having put the decaying terms into  $(C_{(1)} - C_{(2)})$ . We note that  
 95 positioning the first Si atom at  $z$ , the second one at a depth of  $z + \Delta$  is implicitly defining the  
 96 disturbed surface region by setting the first unperturbed atom as the one with three down bonds.

Extending the calculation to the full bulk is straightforward by splitting the crystal in slabs with Si atoms at position (1) or (2), numerating only each double layer by  $n$ , replacing  $z \rightarrow n \cdot d$  and summing the fields coherently over all slabs starting with  $n = 1$  as the first subsurface slab. The procedure is similar to the Ewald Oseen Ansatz<sup>19</sup> for linear optics with the difficulty of using real fields. The outside detected field / intensity is the coherent superposition of the field originating from the surface and the field originating from Si(111) bulk:  $I = \frac{1}{2}c\varepsilon_0|E_{surf} + E_{bulk}|^2$ .

Here we do not treat the field produced by the surface  $E_{surf}$ , where specific models on reconstruction and electronic states would have to be considered. The bulk contribution, however, can be calculated analytically by using computer algebra systems (producing long terms), and also numerically. To determine its relative magnitude, we proceed - in order to show the physics more clearly - by neglecting the phase of the field ( $\simeq$  sign in equ. (4)). This analytic procedure is approximately correct for the case of rather high absorption coefficients, when the field is over-critically damped:

$$P_i^{2\omega,bulk} = \frac{\varepsilon_0}{2} \sum_{jk} \chi_{ijk}^{SL}(2\omega; \omega, \omega) \sum_{n=1}^{\infty} (C_{(1,n)} - C_{(2,n)}) E_j^0(\omega) E_k^0(\omega) \simeq \frac{\varepsilon_0}{2} \frac{(1 - e^{-\Delta(\alpha_{2\omega}/2 + \alpha_\omega)})}{e^{d(\alpha_{2\omega}/2 + \alpha_\omega)} - 1} \sum_{jk} \chi_{ijk}^{SL}(2\omega; \omega, \omega) E_j^0(\omega) E_k^0(\omega) \quad (4)$$

A modified absorption coefficient  $\alpha_{SHG} = \alpha_{2\omega}/2 + \alpha_\omega$  is governing the contribution of the bulk to SHG. For very large, experimentally not achievable,  $\alpha_{SHG}$  (penetration depth of just a few Ås) the formula above yields a vanishing bulk SHG contribution, leaving only the surface effect. As discussed before, in the general case the surface and the bulk field should be added coherently. However, already for harmonic excitation close to the  $E_1$  transition in Si,  $\alpha_{SHG}$  is of the order of  $\simeq 0.02\text{\AA}^{-1}$ , equivalent to penetration depths of just a  $\simeq 120\text{\AA}$  for the exciting wave and  $\simeq 60\text{\AA}$  for the frequency doubled. For  $\alpha_{SHG} = 0.02\text{\AA}^{-1}$  the bulk contribution can give rise to a quarter of the contribution of a single bond for the probably realistic case of setting the first unperturbed atom as the one with three down bonds. If the first unperturbed atom were the one with three upbonds for the Si(111) case, the bulk contribution would give rise to three quarters of the contribution of a single bond. By this calculation it is clear that the bulk contribution cannot be neglected when using SHG as surface analytical tool and can have the same magnitude as the one arising from the surface.

For very small absorption coefficients  $\alpha_{SHG}$ , i.e. almost transparent materials, we find an additional condition, similar to Manley-Rowe relations, which provide the conservation of energy:

Using equ. (4) we use an expansion of the denominator and obtain as leading term  $\frac{\chi^{SL}\Delta}{d}$ , equal to  $\chi^{SL}/4$ . This result cannot be correct, because vanishing adsorption would then imply a rather strong bulk contribution. The wrong result originates from two sources: a) for very small absorption coefficients of the harmonic wave, the hyperpolarisability depends, due to conservation of energy, on the absorption coefficient  $\alpha_\omega$ . Using an ad-hoc Ansatz for the hyperpolarisability to be quadratic -with a small coefficient- in  $\alpha_\omega$ , produces the required result that for vanishing absorption of the harmonic the frequency doubled SHG wave vanishes too. (It also vanishes for linear dependence). b) The second reason comes from the assumption of neglecting the phases. This assumption is not justified any more; for propagation lengths of the order of  $10\mu\text{m}$  phase (mis-)matching (wavevectors  $k_\omega, k_{2\omega}$ ) has to be taken into account in equ. (4).

In order to compare the effects to experiments, we now employ the simplified bond-hyperpolarisability (SBHM) model<sup>11</sup> to calculate the single atom hyperpolarisability  $\chi_{ijk}^{SL}$ . In SBHM the harmonic polarization is given by  $\vec{P}^{2\omega} = \sum_j \beta_{2j} \vec{b}_j \vec{b}_j \bullet \bullet \vec{E} \vec{E} = \chi_2 \bullet \bullet \vec{E} \vec{E}$ , with the bullets denoting outer tensorial products summing over all bonds  $j$ . The hyperpolarisability  $\beta_{2j}$  denotes the nonlinear hyperpolarisability of Si bond, pointing towards the tetrahedra corners. One of the few wavelength dependent data ((p, P) polarization) for a non miscut Si(111) sample have been measured by Kravetsky et al.<sup>20</sup> at a polar angle of incidence (AOI) of  $45^\circ$ .

Before discussing their experimental data we note that for small AOIs - or normal incidence- this model gives rather a 6-fold than a 3-fold symmetry. Assuming a bulk contribution this can be easily explained, because the projection of the field on the 3 bonds is for low AOIs almost identical. In bulk Si, due to the high refractive index, the harmonic wave propagates almost perpendicular to the Si(111) planes and the polarization vector is almost in-plane, also for an external AOI of  $45^\circ$ . The experimental results given in ref.<sup>20</sup> are replotted in the left column of FIG. 3.

Kravetsky et al. measured the same sample (native oxide on Si(111)) at three different frequencies, without modifying the surface. Experimentally, it turns out that the SHG signal is, as a function of the azimuthal angle  $0^\circ - 360^\circ$  either threefold, when the absorption length is small (for a vacuum wavelength of  $\lambda_{0,2\omega} = 266\text{ nm}$ , FIG. 3 (a)) or sixfold when the absorption length is huge (for a vacuum wavelength of  $\lambda_{0,2\omega} = 532\text{ nm}$ , FIG. 3(c)). The fundamental wave has an AOI of  $45^\circ$  in air, within the oxide  $\simeq 29^\circ$  and within Si the AOI is, due to its large refractive index,  $\simeq 9^\circ$ , depending on the wavelength.

We fit all data of ref.<sup>20</sup> with essentially *one* real parameter: This parameter adjusts the relative contribution of the surface with  $AOI = 29^\circ$ , yielding a mainly 3-fold symmetry, and of the

bulk with  $AOI \simeq 9^\circ$ , giving rise to a 6-fold symmetry. A second real parameter mimicking the hyperpolarisability strength  $\beta_2$ , is needed to adjust the arbitrary intensity SHG data. In the right panel of fig. 3 the fits are shown. The SBHM model yields for the up bond a base line shift (plotted in blue) and the contribution of the three down bonds are plotted in red, green and brown. The total intensity is plotted in black. For  $\lambda_{0,2\omega} = 266$  nm only an  $AOI = 29^\circ$  was used, for  $\lambda_{0,2\omega} = 532$  nm a pure bulk contribution was considered and for the intermediate wavelength  $\lambda_{0,2\omega} = 385$  nm approximately 3/4 of the (coherently added) signal arise from the surface ( $AOI \simeq 29^\circ$ ) and 1/4 from bulk. The assignment "surface dipoles" and "bulk dipoles" in the figure stems purely from the different AOIs. The fit for  $\lambda_{0,2\omega} = 532$  nm shows a difference to the experimental data. We assign this difference to the neglect of the wavelength dependence of  $E_{surf}$ . We note that experimental data of Si(111) as a function of the azimuthal angle, taken in another group<sup>21</sup> are almost perfectly matching our predictions. Despite we use only one (bulk-related) parameter, it is clear to us that the surface contribution will be important for certain surface terminations- and furthermore frequency dependent<sup>22</sup>.

Without knowing the absolute SHG intensity it is difficult to determine absolute values for the bulk hyperpolarisability. Despite there have been proposals in the literature (refs.<sup>23,24</sup>) e.g. using steps to separate the "pure" bulk and surface contributions, we propose an unambiguous measurement, separating the harmonic and frequency doubled signals in space. The proposal works for (slightly) dispersive materials and makes use of the different propagation directions, which occur in the material for the harmonic and frequency doubled (back-) radiation. (This back radiation is clear in the Ewald-Oseen picture of coherent radiators). Just using Huygens principle for constructing the planes of equal phase for  $\vec{E}_\omega$  and  $\vec{E}_{2\omega}$  (see FIG. 4) one could determine experimentally the bulk SHG contribution by cutting a Si crystal (e.g. with a focused ion beam) in a shape as shown.

Such a geometry allows to let the  $\vec{E}_{2\omega}$  field pass through the vicinal interface at a different angle as the harmonic field, separating these two. Furthermore, through the vicinal cut surface, only the bulk contributions will contribute to the signal, called  $\theta_{2\omega bulk}$ . This signal is again well separated from the one, where surface and bulk components are in, called  $\theta_{2\omega surf}$ . Knowing the angle of exit and the respective Fresnel coefficient then allows to apply numerically or analytically equations 3 and to determine experimentally the hyperpolarisability. Two experimental challenges have to be overcome: 1) High absorption coefficients  $\alpha_{SHG}$  and small propagation lengths within the crystal will render the radiating region to point-like, and a dispersive source can result; 2) for very small



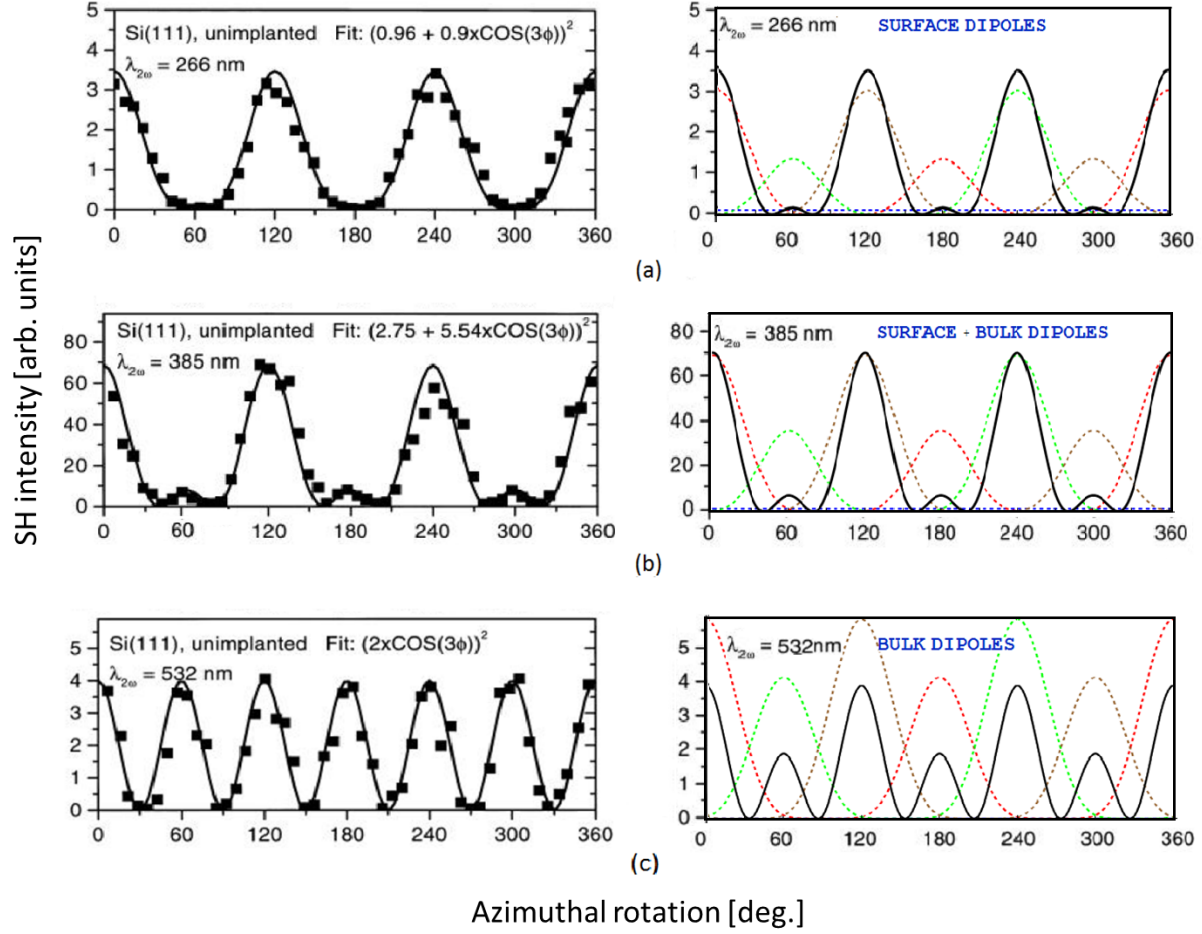


FIG. 3: left column: Measured azimuthal dependence as a function of wavelength (a, b, c.). Data replotted (with permission) from ref.<sup>20</sup>; right column: simulated SBHM data of one slab using one (bulk) hyperpolarisability and two angles of incidence. For  $\lambda_{0,2\omega} = 266$  nm only an  $AOI = 29^\circ$  ( $SiO_2$ ) was used, for the case of  $\lambda_{0,2\omega} = 532$  nm an  $AOI = 11.47^\circ$  for the harmonic wave was used. For  $\lambda_{0,2\omega} = 385$  nm a linear combination of  $AOI = 29^\circ$  and  $AOI = 11.0^\circ$  is used. The total intensity is plotted using black lines and the intensity from the contributing bonds are given in dashed blue (up bond), red (down bond 1), green (down bond 2) and brown (down bond 3)

absorption coefficients the absence of phase matching between the harmonic and second harmonic wave will lead to partially destructive interference.

Summarizing, we show that in the diamond structure dipole allowed bulk SHG response can exist, if two atoms, establishing a symmetric entity, experience different field strengths and thereby

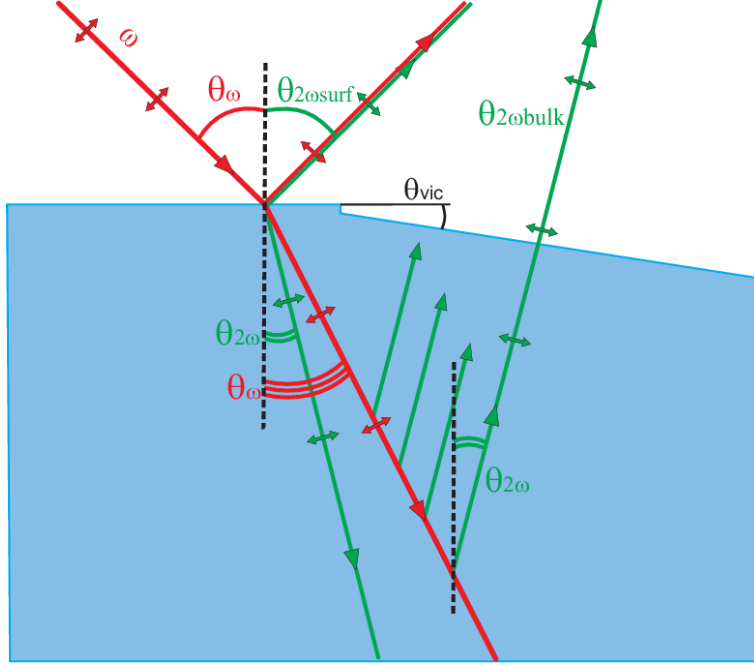


FIG. 4: Proposed geometry for measuring unambiguously the dipolar bulk contribution of SHG. For a harmonic wave of  $\lambda_{0,\omega} = 1064$  nm ( $n=3.64$ ) with an  $AOI = 45^\circ$  and a frequency doubled  $\lambda_{0,2\omega} = 532$  nm ( $n=4.14$ , penetration depth  $\simeq 1.3\mu\text{m}$ ) and for  $\theta_{vic}$  of  $9.8^\circ$  the SHG wave passes the vicinal surface without being refracted ( $\theta_{2\omega bulk} = 0^\circ$ ), but the harmonic is refracted  $\theta_\omega = 5.8^\circ$  to the right. So, the frequency doubled wave, which contains surface and bulk contributions, is approximately  $35^\circ$  separated from the field only containing the bulk contribution.

radiated harmonic field does not fully cancel. The dipole allowed bulk SHG originates then due to the finite absorption length of the electric field in material. The magnitude of this effect is of the order of a single bond and can contribute the same signal as e.g. a surface atom. We compare with available wavelength dependent SHG data, whose azimuthal dependence can be well modeled by just using one parameter. Finally we propose a measurement scheme capable of unambiguously separating bulk and surface effects.

*Acknowledgements:* We thank Norbert Esser and Siegfried Bauer for valuable comments on the manuscript. The financial support by the Federal Ministry of Economy, Family and Youth and the

National Foundation for Research, Technology and Development is gratefully acknowledged.

---

\* email: kurt.hingerl@jku.at

<sup>1</sup> B. Gokce, E. J. Adles, D. E. Aspnes, and K. Gundogdu. *PNAS*, 107(41):17503–17508, 2010.

<sup>2</sup> C. Schrieffer, C. Bohley, and R. B. Wehrspohn. *Opt. Lett.*, 35(3):273–275, 2010.

<sup>3</sup> M. Cazzanelli, F. Bianco, E. Borga, G. Pucker, M. Ghulinyan, E. Degoli, E. Luppi, V. Veniard, S. Ossicini, D. Modotto, S. Wabnitz, R. Pierobon, and L. Pavesi. *Nature Materials*, 11:148–154, 2012.

<sup>4</sup> J. F. McGilp. *Journal of Physics: Condensed Matter*, 22(8):084018, 2010.

<sup>5</sup> K. Sahu, K. B. Eisenthal, and V. F. McNeill. *J. Phys. Chem. C*, 115(19):9701–9705, 2011.

<sup>6</sup> F. X. Wang, F. J. Rodriguez, W. M. Albers, R. Ahorinta, J. E. Sipe, and M. Kauranen. *Phys. Rev. B*, 80:233402, 2009.

<sup>7</sup> P. Guyot-Sionnest and Y. R. Shen. *Phys. Rev. B*, 38:7985–7989, 1988.

<sup>8</sup> W. S. Kolthammer, D. Barnard, N. Carlson, A. D. Edens, N. A. Miller, and P. N. Saeta. *Phys. Rev. B*, 72:045446, 2005.

<sup>9</sup> H. J. Peng, E. J. Adles, J.-F. T. Wang, and D. E. Aspnes. *Phys. Rev. B*, 72:205203, 2005.

<sup>10</sup> M. Corvi and W. L. Schaich. *Phys. Rev. B*, 33:3688–3695, 1986.

<sup>11</sup> G. D. Powell, J.-F. Wang, and D. E. Aspnes. *Phys. Rev. B*, 65:205320, 2002.

<sup>12</sup> R. W. Boyd. *Nonlinear Optics*. Academic Press, 2003.

<sup>13</sup> Y. R. Shen. *Nature*, 337:519–525, 1989.

<sup>14</sup> N. Bloembergen, R. K. Chang, S. S. Jha, and C. H. Lee. *Phys. Rev.*, 174(3):813–822, 1968.

<sup>15</sup> G. New. *Introduction to Nonlinear Optics*. Introduction to Nonlinear Optics. Cambridge University Press, 2011.

<sup>16</sup> G. Kresse and D. Joubert. From ultrasoft pseudopotentials to the projector augmented-wave method. *Phys. Rev. B*, 59:1758–1775, Jan 1999.

<sup>17</sup> V.M. Agranovich and V.L. Ginzburg. *Spatial dispersion in crystal optics and the theory of excitons*. Number Bd. 18 in Interscience monographs and texts in physics and astronomy. Interscience Publishers, 1966.

<sup>18</sup> J. E. Mejia, C. Salazar, and B. S. Mendoza. *Revista Mexicana de Fisica*, 50(2):134–139, 2004.

<sup>19</sup> H. Fearn, D. F. V. James, and P. W. Milonni. *Am. J. Phys.*, 64(8):986–995, 1996.

<sup>20</sup> I.V. Kravetsky, L.L. Kulyuk, J.F. McGilp, M. Cavanagh, S. Chandola, J. Boness, G. Marowsky, and

- 230 F. Harbsmeier. *Surf. Sci.*, 402-404:542–546, 1998.
- 231 <sup>21</sup> F. Ito and H. Hirayama. *Phys. Rev. B*, 50:11208–11211, 1994.
- 232 <sup>22</sup> S.A. Mitchell, M. Mehendale, and D.M. Villeneuve. *Surface science*, 488(3):367–378, 2001.
- 233 <sup>23</sup> G. Lüpke, D. J. Bottomley, and H. M. van Driel. *J. Opt. Soc. Am. B*, 11(1):33–44, 1994.
- 234 <sup>24</sup> J. F. McGilp. *Journal of Physics: Condensed Matter*, 19(1):016006, 2007.